Geophys. J. R. astr. Soc. (1978) **52**, 45–64

A detailed rock magnetic and opaque mineralogy study of the basalts from the Nazca Plate

H. Paul Johnson *Department of Oceanography, University of Washington, Seattle, Washington 98195, USA*

James M. Hall *Department of Geology, Dalhouse University, Halifax, Nova Scotia, Canada*

Received 1977 July 18; in original form 1977 April 15

Summary. The penetration of igneous basement in the Nazca Plate during DSDP Legs 16 and 34 provided samples of both fine-grained pillow-basalt and coarse-grained massive flow units. The magnetic mineral in these basalt samples is initially a titanomagnetite ($Fe_{3-x}Ti_xO_4$) with a narrow range of composition of $x = 0.62 \pm 0.05$. Subsequent to formation, the titanomagnetite grains are generally subjected to low temperature oxidation to titanomaghemite with a corresponding rise in Curie temperature from the initial values of 120–150°C up to a maximum of 400°C. Both grain size and low-temperature oxidation state play important, and interrelated, roles in controlling the intensity and stability of magnetic remanence and other magnetic properties. Overall grain size can, in some cases, be related to oxidation state since some sections of the relatively impermeable massive flows can remain unoxidized for as long as 40 Myr while pillow basalts are extensively oxidized within ½ Myr. Low-temperature alteration in turn effects magnetic grain size since oxidation and subsequent Fe cation migration results in grain subdivision by the formation of shrinkage cracks. A five-stage sequence of the microscopic changes that are associated with progressive low-temperature oxidation is proposed and illustrated with photomicrographs from these basalt samples.

A hierarchy in the intensity of magnetic remanence may exist with unoxidized pillow basalts having a much higher intensity and oxidized pillow basalts having a much lower intensity than the massive flow units. While pillow basalts are relatively immune to the addition of secondary components of magnetization, the coarse-grained massive flows readily acquire components of viscous remanence. Although they oxidize much more slowly than pillows, when oxidation does take place, components of chemical remanence can be acquired by the multi-domained grains in the massive flow units.

1 Introduction

Leg 34 of the Deep Sea Drilling Project penetrated a total of 105 m of the igneous oceanic crust at three sites in the Nazca Plate. A total of 41 basalt samples were taken for magnetic

and opaque mineralogy studies and included both fine-grained pillow and coarse-grained holocrystalline material (Fig. 1). In addition, four samples were taken from the massive basalt core of DSDP Leg 16, site 157, which was also situated within the Nazca Plate. The palaeomagnetic data from these samples has been reported earlier (Johnson & Hall 1976), and in this study, we report the results of an intensive rock magnetic and opaque mineralogy investigation. It is hoped that a detailed examination of these parameters would provide some insight into the magnetic properties of submarine basalts, in general, and perhaps shed some light on the origin and evolution of the upper part of oceanic igneous layer 2.

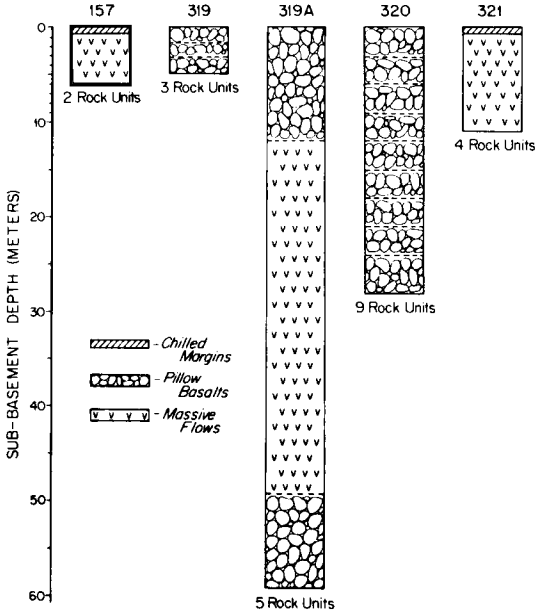

Figure 1. Lithological units for the four drill sites in the Nazca Plate.

2 Experimental methods

The magnetic properties determined for these submarine basalt samples were: saturation magnetization, Curie temperature, weak field susceptibility, median demagnetizing field, and natural remanent magnetization. The oxide petrography, the oxidation state, and the bulk titanomagnetite content were studied by reflected light microscopy. The saturation magnetization and Curie temperatures of the samples were measured in a Cahn R-100 electrobalance using a 7.5 kilogauss (6.0×10^5 A/m) electromagnet. The heating rates were of the order of 100°C/min, and heating was done at atmospheric pressure with nitrogen as the residual gas. Repeated purging of the furnace with nitrogen prior to heating insured that the effective oxygen fugacity was below that which would oxidize the titanomagnetite grains.

Weak-field susceptibility was measured using a commercial bridge (Soil Test Model MS3). Remanence measurements were made on a Schonstedt SSM1 spinner magnetometer. Opaque mineralogy studies were conducted by the authors at Dalhousie University and by L. K. Fink at the University of Maine. The photomicrographs in the paper were taken using the facilities at the US Geological Survey at Golden, Colorado.

Table 1. Measured compositions of titanomagnetite grains from Pacific and Atlantic basalt samples.

Site	Location	x value (± 1 SD) in $Fe_{3-x}Ti_xO_4$	Number of analyses	Technique used	References
DSDP 319	All in Nazca Plate	0.65 ± 0.05	42 grains from 23 samples	Microprobe	1, 2, 3, 4
DSDP 320		0.54	1 grain from 1 sample	Microprobe	2
DSDP 321		0.66 ± 0.01	11 grains from 8 samples	Microprobe	1, 2, 4
DSDP 157	Nazca	0.63	1 grain from 1 sample	Microprobe	5
DSDP 169	Central Pacific Basin	0.57 ± 0.04	5 analyses from 5 samples	Microprobe	6
AM 49	Mid-Atlantic Ridge	0.68	1 sample	X-ray	7
MOHOLE EM-7	Guadalupe Site	0.67	1 sample		
DSDP 342	Norwegian Sea	0.65 ± 0.03	3 samples	Microprobe	8
DSDP Leg 15	Caribbean Sea	0.54 ± 0.06	7 samples	Microprobe	9
DSDP 395A	Mid-Atlantic Ridge at 23° N	0.60 ± 0.04	237 analyses of 50 grains from 10 samples	Microprobe	10

Average of all sites: $x = 0.62 \pm 0.05$.

References

1. Donaldson, Brown & Reid (1976). 2. Mazzulo, Bence & Papike (1976). 3. Bunch & La Borde (1976). 4. Ridley & Ajdukiewicz (1976). 5. Yeats *et al.* (1973). 6. Myers *et al.* (1975). 7. Ozima, Joshima & Kinoshita (1974). 8. Ridley, Perfit & Adams (1976). 9. Bence, Papike & Ayuso (1975). 10. Johnson & Melson (1977).

3 Magnetic mineralogy of submarine basalts

The major magnetic mineral in almost all submarine basalts recovered to date is a member of the titanomagnetite solid solution series that is either unoxidized or, more commonly, has undergone various stages of post-eruptive low-temperature alteration. Two variables, x and z, are needed in order to define the composition of this type of magnetic mineral (Fig. 2). Upon initial eruption, the mineral that is originally formed is a member of the solid solution series between magnetite and ulvospinel, which is defined by 'x' in the relationship $Fe_{3-x}Ti_xO_4$. Table 1 shows a compilation of values of x for samples from both the Pacific and the Atlantic Oceans. While there are not a large number of analyses, there is not much variation around the average value of $x = 0.62 \pm 0.05$. There does not seem to be any systematic difference between the sites, which vary in age from very recent to 40 Myr old. This value agrees very closely with the value of $x = 0.64$ obtained for 49 analyses of continental tholeiite basalts described by Petersen (1976). Using geochemical arguments, Carmichael & Nicholls (1967) predict a value for x between 0.85 and 0.50 for titanomagnetites crystallizing from basaltic liquids. The value of x is dependent upon the relative order of silicate and oxide crystallization and, therefore, will depend on the temperature, oxygen fugacity, and composition of the basaltic magma. The narrow range of titanomagnetite composition generally found in the igneous submarine basement rocks seems to reflect both a narrow range of conditions present during oceanic igneous crust formation and the fact that in tholeiite basalts, titanomagnetite is one of the last mineral phases to crystallize.

The second variable that must be determined in order to characterize titanomagnetite that has been altered to titanomaghemite is the fraction of the original ferrous ions that are

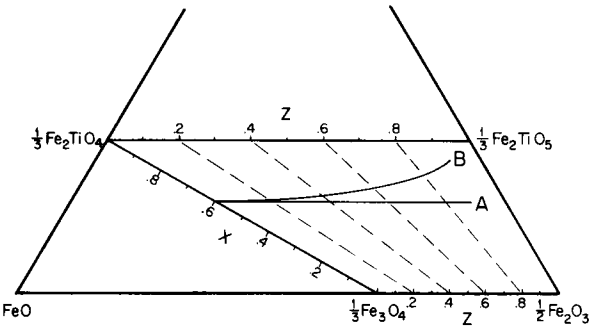

Figure 2. The relevant part of the familiar $FeO-TiO_2-Fe_2O_3$ ternary diagram. Characterization of the titanomagnetite–titanomaghemite series by x and z, as described in the text, is shown. Line A shows the progressive low-temperature oxidation where the Fe/Ti ratio is constant. Line B is an example of low-temperature oxidation where the Fe/Ti ratio is decreasing by iron migration out of the original crystal lattice and into the surrounding silicates.

oxidized to ferric ions. This parameter, z, can be expressed as

$$Fe^{+2} + \tfrac{1}{2}zO_2 \rightarrow zFe^{+3} + (1 - z)\,Fe^{+2} + zO^{-}$$

with $z = 0$ describing completely unoxidized and $z = 1$ completely oxidized conditions, respectively (O'Reilly & Banerjee 1967; Readman & O'Reilly 1971). Characterization of the titanomagnetite–titanomaghemite series in submarine basalts by x and z allows the correlation of magnetic properties with mineral composition during progressive alteration.

Fig. 2 shows the relationship of the two variables, x and z, on the familiar ternary diagram of iron–titanium oxides. The two parameters can be determined by measuring Curie temperature and either the lattice parameter by X-ray diffraction or the iron and titanium content by electron microprobe analysis. In practice, the latter method is limited to coarse-grained basalts (median titanomagnetite grain size of 20 μm and larger), and even then some degree of spreading of the electron beam into the adjacent silicates can occur (Ade-Hall, Fink & Johnson 1976). The diagram is normalized so that oxidation without any change in the Fe/Ti ratio will be a horizontal straight line, as in A. Line B represents a possible oxidation path where the iron is selectively migrating out of the titanomaghemite lattice during oxidation. There is growing evidence that low-temperature alteration of titanomagnetite involves a diffusion of some of the Fe^{+2} cations away from the original lattice site into the surrounding silicates during oxidation to Fe^{+3} (Johnson & Melson 1977). This would result in a decrease in the Fe/Ti ratio for the remaining oxide phases and an oxidation path similar to B rather than A (Prévot, Rémond & Caye 1968; Marshall & Cox 1972; Grommé & Mankinen 1976; Ade-Hall, Johnson & Ryall 1976).

4 Results

Fig. 1 shows the basement lithology for the Nazca Plate drill holes. The presence of both fine grained material and massive flow units in the same holes (319 and 321) allows us to compare the magnetic properties and to estimate the similarities and differences in evolution of these two types of lithological units. Hole 320 consists entirely of pillow basalt units.

4.1 CONCENTRATION OF MAGNETIC MINERALS

Two independent techniques were used in this study to determine the volume percentage of the magnetic mineral: first, by a direct measurement of the titanomagnetite grain volume

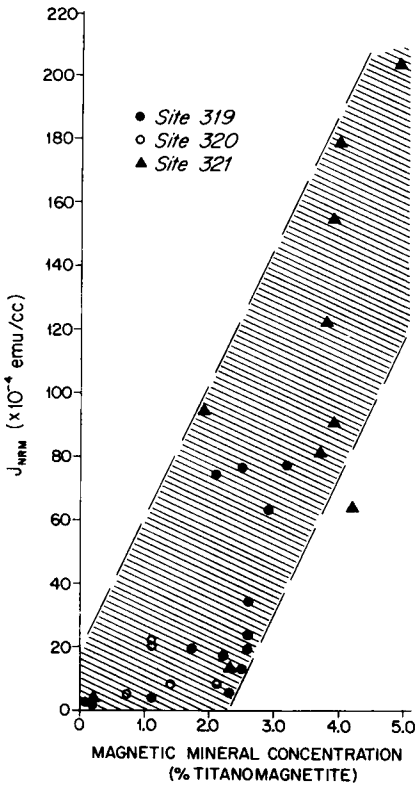

Figure 3. The relationship between intensity of magnetic remanence and the concentration of the magnetic mineral in each individual rock sample. Grain size, oxidation state, and grain interactions are not taken into account in this figure and are probably responsible for the relationship being only broadly linear.

using reflected light-microscope observation of polished sections (100 grain count per sample) and, second, an indirect calculation from the saturation magnetic moment (J_s) of the whole rock. In the latter, an estimate of the specific saturation magnetization for the particular value of z involved is made from the Curie temperature and the contours given in Readman & O'Reilly (1972, Fig. 2). The range of concentration of magnetic minerals in the samples in this study was roughly within one order of magnitude (volume percent of titanomagnetite ranged between 0.2 and 5 per cent), with the pillow basalts averaging about 1 per cent or less and the massive flow units usually between 2 and 3 per cent, with some higher values. Fig. 3 shows the relationship between volume percentage of the magnetic mineral and intensity of remanence corrected for the addition of secondary remanence, for the three sites. While there is a general increase in intensity with increasing content of magnetic mineral, the relationship appears to be only broadly linear, and there are clearly other variables, like grain size, which must be taken into account. Some of the scatter in Fig. 3 should be attributed to the difficulty in making accurate estimates of the magnetic mineral concentration as well as the possible addition of secondary components to the NRM intensity.

4.2 SATURATION MAGNETIZATION

Fig. 4(a) shows the plot of the intensity of remanence against the values for the whole rock saturation moment. Only those samples with clearly identifiable single components of NRM

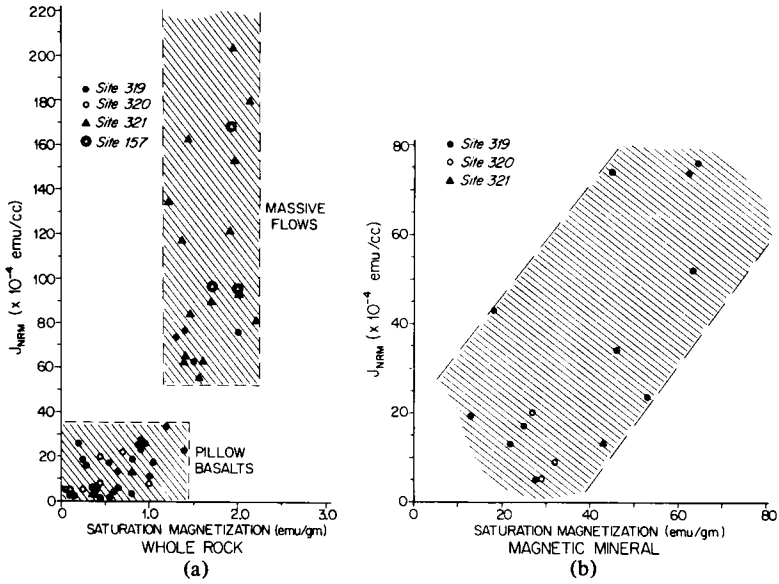

Figure 4. Intensity of magnetic remanence as a function of saturation magnetization. (a) The variation of intensity with whole rock saturation magnetization. (b) The dependence of remanence intensity of the saturation magnetization of the specific magnetic mineral in each sample (obtained by dividing J_S (rock) by the concentration). (a) Shows only the separation of pillows and massive flow units into two groups, while (b) shows that intensity is broadly dependent on J_S (mineral).

were used. Since the saturation magnetization, J_S, of the whole rock sample is proportional to the product of the saturation moment of the magnetic mineral present and its concentration, it is possible to obtain the saturation moment of the specific magnetic mineral by dividing the saturation moment of the rock by the percentage concentration of the mineral. Fig. 4(b) shows a plot of NRM intensity against the calculated value of J_S of the magnetic mineral. In both Fig. 4(a) and (b) there is general increase in NRM intensity with increasing J_S, but the large amount of scatter in the data conceals any identification of the functional dependence. If all other parameters are held constant, the intensity of magnetic remanence should be linearly proportional to both the saturation magnetization and the concentration of the magnetic mineral. Fig. 3 shows that, while this is roughly true for concentration, Fig. 4(a) and (b) indicate that it is true only in the most general sense for J_S. Some of the scatter in Fig. 4 must be due to the uncertainty in determining the values of the experimental data, particularly the mineral concentration, but the poor correlation may also indicate that the intensity of remanence is also controlled by factors other than the saturation moment.

4.3 CURIE TEMPERATURE

An unoxidized titanomagnetite of the composition ($x = 0.62 \pm 0.05$) has a Curie temperature of between 120 and 150°C with a reversible $J_S(T)$ curve when heated in a non-oxidizing environment. Previous studies on the very young rocks from Mid-Atlantic Ridge have found that other unaltered submarine basalts have Curie temperatures in the range 120–150°C with a continuous rise in Curie temperature with progressive low-temperature oxidation up to maximum values of about 400°C (Schaeffer & Schwarz 1970; Johnson & Atwater 1977). Curie temperatures were determined on all samples from the four sites in this study and ranged from 120°C to just below 400°C. Samples within the range 120–175°C showed reversible heating and cooling curves, while the higher Curie point samples (greater than

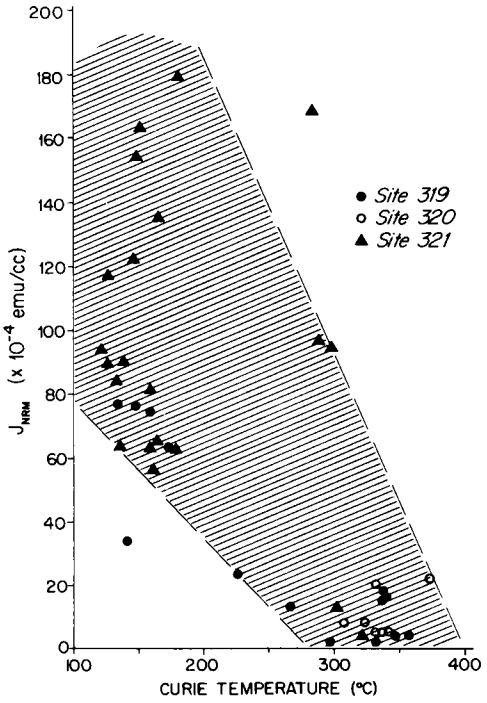

Figure 5. The dependence of magnetic intensity on Curie temperature. While the scatter is sufficiently large to obscure any functional dependence, the high intensity values are clearly associated with the low Curie points and Curie temperatures above 300°C are associated with low magnetic intensities. Since Curie temperature is related to degree of low-temperature oxidation, this figure indicates that the amount of oxidation plays an important role in controlling the magnetic intensity.

225°C) showed the characteristic breakdown of titanomaghemite upon heating. Work on the Mid-Atlantic Ridge basalts recovered during DSDP Legs 37 and 45 showed that reversible $J_s(T)$ curves can occur in samples that are slightly oxidized with Curie temperatures as high as 200°C (Hall & Ryall 1977; Johnson 1977a). One basalt sample from this Nazca Plate study (16-157–49-2; 135 to 137) showed a reversible Curie temperature of 490°C and subsequent microscopic examination confirmed the presence of a low titanium magnetite with exsolved ilmenite lamellae – evidence of high-temperature oxidation.

Fig. 5 shows the correlation of intensity of remanence and Curie temperature. Clearly, the high intensity values are associated with low Curie points, near 120–150°C, and low intensity values are associated with high Curie temperatures, near 400°C. This indicates that low-temperature oxidation plays an important role in controlling the intensity of magnetic remanence.

Fig. 6 shows a plot of the magnetic mineral saturation moment (J_s (rock) divided by concentration) as a function of Curie temperature. A factor of from 5 to 10 separates the intensities of little and highly oxidized samples and thus is a true measure of the control on remanence intensity by low-temperature oxidation. As has been determined from other studies (Readman & O'Reilly 1972; Ozima & Ozima 1971; Johnson & Merrill 1973), low-temperature oxidation of titanomagnetite produces both an elevation of Curie point above the initial low values and a corresponding decrease in the saturation magnetization. It should be noted in Fig. 6 that the values of J_s for the unoxidized titanomagnetites with compositions close to $x = 0.62$ are substantially greater (average twice as high) than the values of 25 emu/gm (25 A m^2/kg), which has been obtained for synthetic titanomagnetites of the

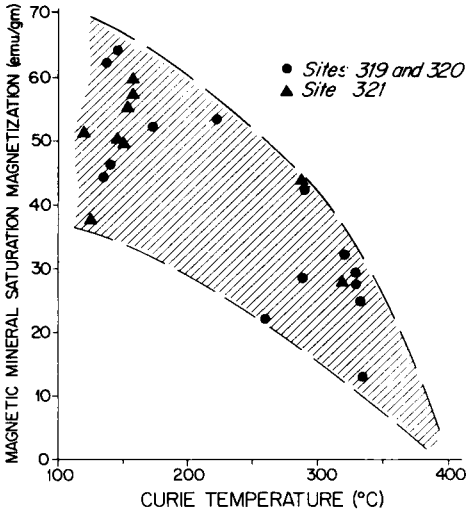

Figure 6. The relationship between the saturation magnetization of the magnetic mineral and Curie temperature. This decrease in J_s (mineral) with increasing oxidation has been both predicted by various cation-distribution models and observed in progressively oxidized pillow basalts.

same composition (Readman & O'Reilly 1972). This could be due either to a cation order–disorder phenomena in the natural samples that is not present in the synthetic samples or to the presence of a large quantity (approximately 50 per cent of the total volume) of sub-microscopic titanomagnetite grains that are undetected even at the limit of optical resolution.

4.4 GRAIN SIZE

The recovery, at sites 319 and 321, of both relatively coarse grained and fine grained pillow basalts allows us to compare the effects of grain size on the magnetic properties. All of the pillow basalt material was at least partially oxidized while the coarse-grained massive flow units were in either the oxidized or unoxidized state. Fig. 7 shows the relationship between

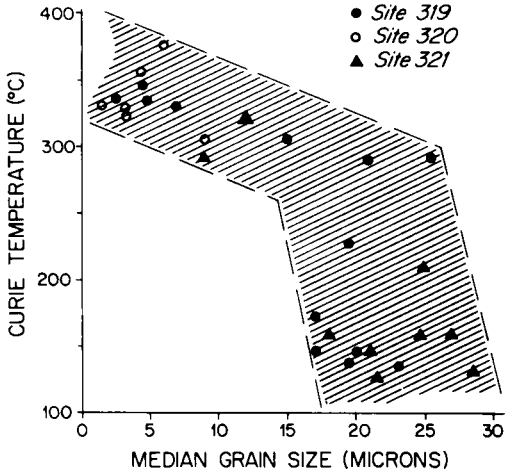

Figure 7. Curie temperature as a function of grain size. The dividing line between pillow basalts and massive flows is not clearly defined but can be taken as between 10 and 15 μm. This figure shows that the relatively impermeable massive flows are much less oxidized than the more permeable pillow basalt units of the same age.

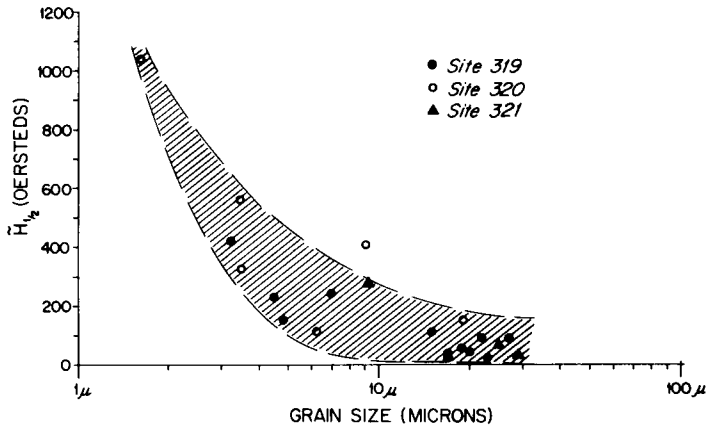

Figure 8. The dependence of coercivity on magnetic grain size. Coercivity is expressed as median demagnetizing field, or the peak alternating demagnetizing field that reduces the intensity of remanence by one half. If this figure is compared with Fig. 12, it would appear that the magnetic minerals in the samples in most of this study are all larger than single-domain in size.

grain size and Curie temperature. Again, within the scatter of the data, the smaller, fine-grained pillow basalts are much more oxidized than the coarse-grained, massive flow material.

Fig. 8 shows the plot of grain size versus median demagnetizing field for the Nazca Plate samples with an increase in median demagnetizing field with decreasing grain size. As expected, the fine-grained pillow basalt material shows a higher stability against AF demagnetization than the coarser grained material. There is a problem of separation of variables since this could be due to either grain size or the oxidation state. The fine-grained material is, in general, more oxidized than the coarser material, and it has been established previously that increasing the oxidation state in titanomagnetite grains also increases the coercivity up to the upper limit of single domain grain size (Johnson & Merrill 1973; Johnson & Ade-Hall 1975).

Fig. 9 shows the relationship between grain size and NRM intensity. There seems to be a clear division into three categories: oxidized pillow basalts, and oxidized and unoxidized massive flow material (no unoxidized pillow material was recovered in Legs 16 and 34). In order to compare the magnetic properties of these different types of material, Table 2 shows some of the averages for unoxidized pillow basalts from the FAMOUS area compared with that from the current study of Nazca Plate material. Although the average remanent intensity for the unoxidized massive flows may be a minimum value due to the presence of opposing secondary components, the *in situ* value is unlikely to approach that of the unoxidized pillow basalts.

5 Susceptibility

The measurement of initial susceptibility is important in submarine basalts in order to determine the *in situ* intensity of the magnetization induced in the present field. Fig. 10 shows the variation of susceptibility with the parameters saturation magnetization, grain size, and Curie temperature. We have previously shown (Johnson & Hall 1976) that these samples show a correlation between J_{NRM} and susceptibility with decreasing susceptibility associated with the decreasing intensity of magnetization. *The slope of the correlation line insures that, for these samples at least, the values of the ratio of remanence intensity to induced component* (Q) *will always be greater than 1 during progressive low-temperature oxidation and the*

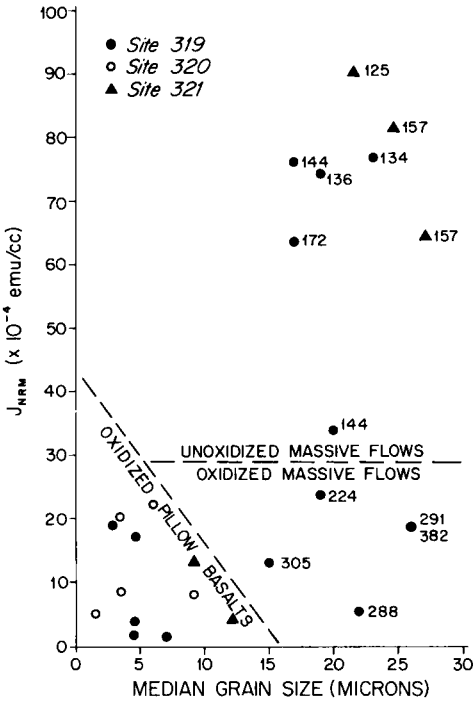

Figure 9. The relationship between intensity of remanence and grain size. The numbers next to the data points are Curie temperatures in degrees centigrade. The field can be divided into the three areas shown, with unoxidized pillow basalts having substantially higher remanence intensities (Table 2).

Table 2. Comparison of pillow basalt and massive flow units in the oxidized and unoxidized state.

Lithological classification	Remanent intensity (1×10^{-3} emu/cm^3=1 A/m)	Weak-field susceptibility (1×10^{-3} emu/cc/oe=1 A/m/oe)	Curie temperature (°C)	Median demagnetizing field Oersteds	$\times 10^3$ A/m
Unoxidized pillow basalts*	24	3.5	145	190	15.1
Unoxidized massive flows†	6.5‡	0.84	147	64	5.1
Oxidized massive flows†	1.2	0.13	290	167	13.3
Oxidized pillow basalts†	0.86	0.086	340	258	20.5

*From the FAMOUS area of the Mid-Atlantic Ridge (Johnson & Atwater 1977).
† This study.
‡ Due to the addition of opposing secondary components, this is probably a minimum value (Ade-Hall & Johnson 1976a).

remanence will always dominate. Fig. 10(a) shows the relationship between saturation magnetization and weak field susceptibility. The range of variation of susceptibility seems to be much larger than the simple linear relationship that would be expected if the parameters other than concentration were held constant. Fig. 10(b) shows a general increase in susceptibility with increasing grain size, but, since oxidation also clearly varies with grain size (Fig.

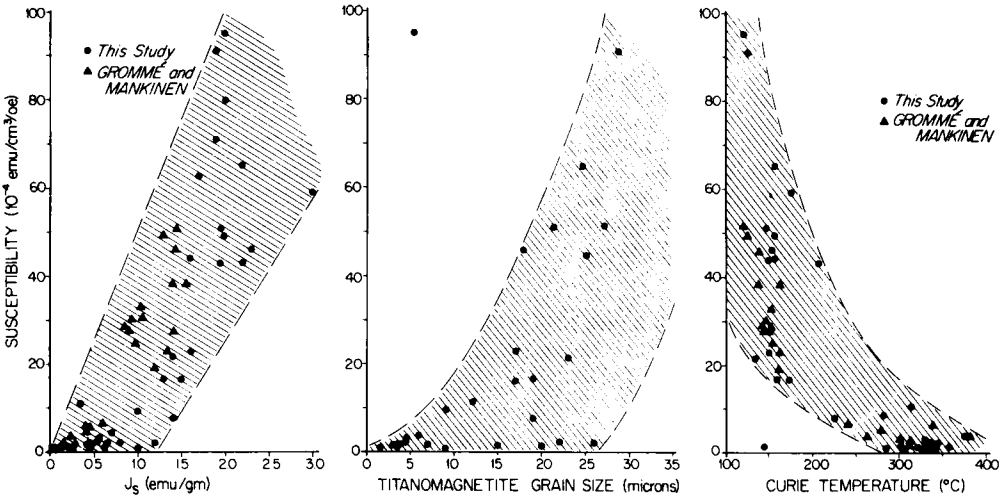

Figure 10. The variation of weak-field susceptibility with saturation moment (J_S), grain size, and Curie temperature. (a) The dependence of susceptibility on the saturation magnetization of the whole rock sample and includes data from this study and from Grommé & Mankinen (1976) on samples from the same drill cores. (b) Has a smaller number of samples (grain size was not determined on the entire suite of samples) and illustrates the general increase in susceptibility with increasing grain size. This increase is probably related to both the decrease in coercivity (Fig. 8) and the increase in saturation magnetization (Fig. 6) that accompany increasing grain size. (c) The strong decrease in susceptibility with increasing Curie temperature and the corresponding increase in degree of low temperature oxidation, again including samples from this study and from Grommé & Mankinen (1976).

7), there is again a problem of separation of variables. Finally, Fig. 10(c) shows that, as for J_{NRM}, weak-field susceptibility shows a general decrease with increasing Curie temperature and associated low-temperature oxidation.

6 Secondary components of magnetization

The ability of the coarse-grained massive flow samples to acquire secondary components of magnetization has already been reported in detail earlier. In particular, these samples seem to be able to readily acquire viscous remanent magnetization (Lowrie & Kent 1976; Denham & Guertler 1976; Tarasiewicz, Tarasiewicz & Harrison 1976), a vertical component of remanence during drilling (Ade-Hall & Johnson 1976a), rotational remanent magnetization (Grommé & Mankinen 1976; Ade-Hall & Johnson 1976b), and chemical remanent magnetization (Grommé & Mankinen 1976; Johnson & Hall 1976). We will not discuss these particular studies further, except to comment in general about the ability of submarine basalts to acquire chemical remanent magnetization (CRM) during low-temperature oxidation.

It would appear that there are sometimes certain circumstances present within rock samples which can prevent the acquisition of a CRM component parallel to the external field even though the magnetic mineral is undergoing drastic physical changes in the presence of an external magnetic field. Table 3 gives a summary of two different types of grain sizes of submarine basalts along with some artificial magnetite samples and their ability to acquire a CRM component during low-temperature oxidation. It would seem clear from the studies listed in Table 3 that fine-grained pillow basalts have the unexpected property of not being able to acquire a CRM component in the direction of the external field, even with substantial amounts of oxidation, at the ambient temperatures present on the sea floor. This resist-

Table 3. Ability of magnetic minerals to acquire chemical remanent magnetization.

Type of magnetic mineral	Oxidation temperature 4°C to 50°C	50°C and above
Fine-grained pillow basalts: titanomagnetite grain size; 1–10 μm	No CRM (1, 2, 3)	CRM (4, 5)
Coarse-grained massive flows: titanomagnetite grain size; 10–100 μm	CRM (6, 7)	Not done
Single domain magnetite rods 0.4 × 0.04 μm	Not done	No CRM (8)
Equi-dimensional magnetite cubes 0.2 μm	Not done	CRM (9)
Coarse-grained magnetite particles 2–44 μm	Not done	CRM (9)

References

(1) Marshall & Cox 1972; (2) Ryall & Ade-Hall 1975b; (3) Johnson & Atwater 1977; (4) Marshall & Cox 1971b; (5) Johnson & Merrill 1973; (6) Johnson & Hall 1976; (7) Grommé & Mankinen 1976; (8) Johnson & Merrill 1974; (9) Johnson & Merrill 1972.

ance to CRM acquisition is also shared by single domain magnetic needles when oxidized at temperatures of 100 and 200°C. This inability to acquire a CRM component during extensive low-temperature oxidation could be due either to a pinning of the magnetic remanence by a strong shape anisotropy of the magnetic grains (as with the long, thin, artificial magnetite rods) or by a positive exchange coupling between the unoxidized and oxidized magnetic phases (Johnson & Merrill 1974).

In magnetic grains that are large enough to allow domain wall motion, domain wall readjustment during oxidation could allow an uncoupling of the unoxidized and oxidized phases and a CRM component would be acquired. Thus, we have the situation that, while coarse-grained massive flows are much more resistant to oxidation than fine-grained pillow basalts due to their relative impermeability to sea water, these massive flow units can acquire secondary magnetic components, both viscous and chemical, and as a consequence, post-formation changes in magnetic remanence directions. Pillow basalts are much more resistant to these magnetic direction changes.

7 Opaque mineralogy

In the previous section, we have discussed how some of the magnetic properties have varied with grain size, oxidation state, and concentration. While some of the variation in magnetic properties can be attributed to the simple oxidation of ferrous to ferric ions in the conversion of titanomagnetite to titanomaghemite, some of the parameter variation seems to require at least one and perhaps several additional factors.

All samples studied were examined in polished section using an incident light microscope. Unlike the standard techniques for the preparation of thin sections, these samples were prepared and polished completely at room temperature. This is important since even the moderate heating of 200°C normally used to prepare microscope samples can cause substantial phase changes in the opaque mineralogy of submarine basalts (Johnson & Merrill 1973; Ryall & Ade-Hall 1975a).

Fig. 11 shows a schematic diagram of the microscopic changes associated with progressive low-temperature oxidation. Since low-temperature oxidation is not a uniform process, the Curie temperatures shown with each stage are only representative of the samples in this study and should be interpreted only generally (e.g. submarine basalt samples with Curie temperatures between 300 and 400°C will not always show the features of Stage 4).

Plates 1–5 show a sequence of samples selected to show progressive stages of oxidation at low temperature. Plate 1 shows a typical example of Stage 1 unaltered titanomagnetite grains. These high-titanium, unoxidized, titanomagnetite grains are an homogeneous medium

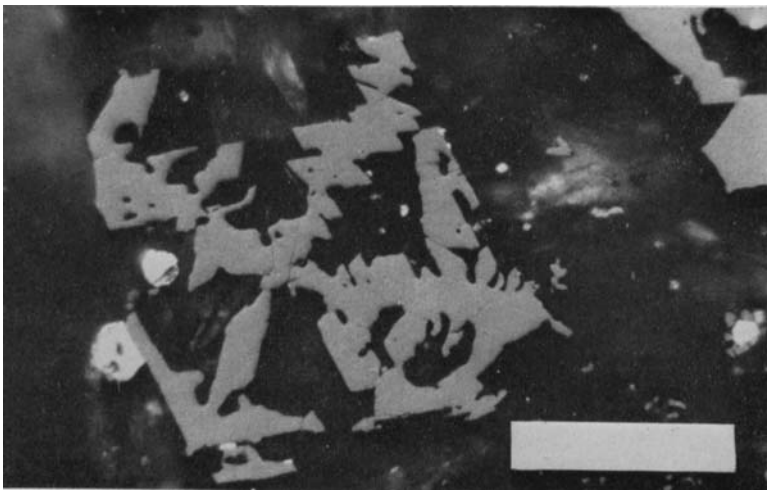

Plate 1. A grain of unoxidized titanomagnetite from sample 34-321-14-2 : 12 to 15. The white bar in the plate is 50 μm long.

[*facing page* 56]

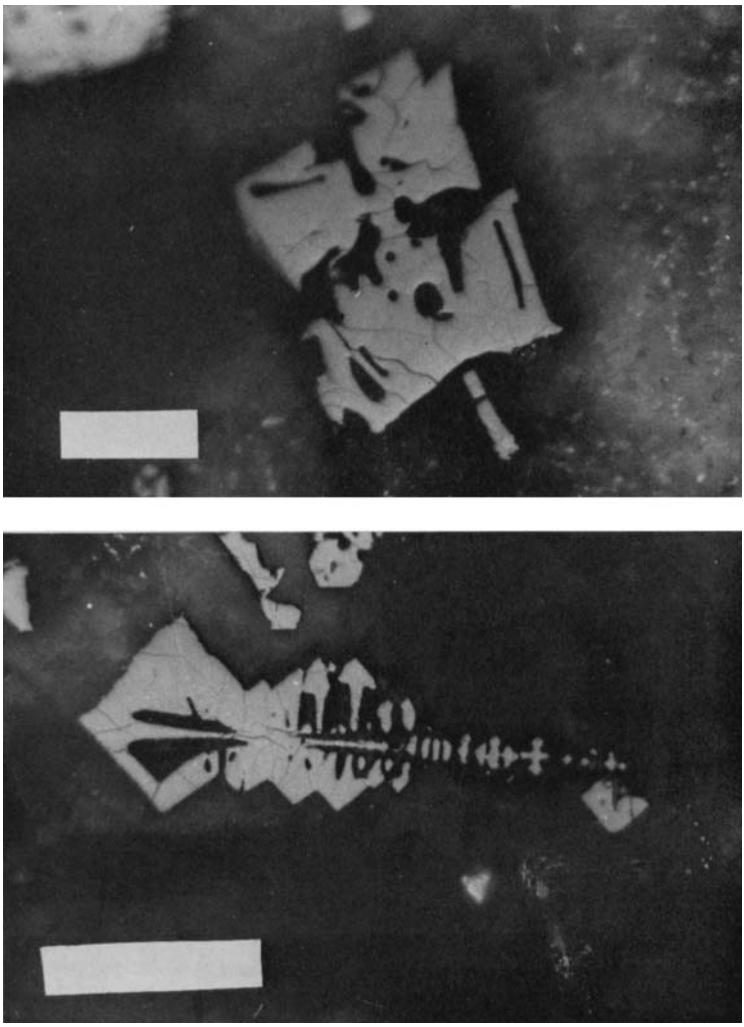

Plate 2. Two grains of partially oxidized titanomaghemite from sample 34-319A-1-1 : 39 to 42. These samples show the fine-scale cracking that is typical of the end of Stage 2 or the beginning of Stage 3. These grains have probably already passed through the initial discoloration associated with the onset of Stage 2. The white bars in these plates are 25 μm.

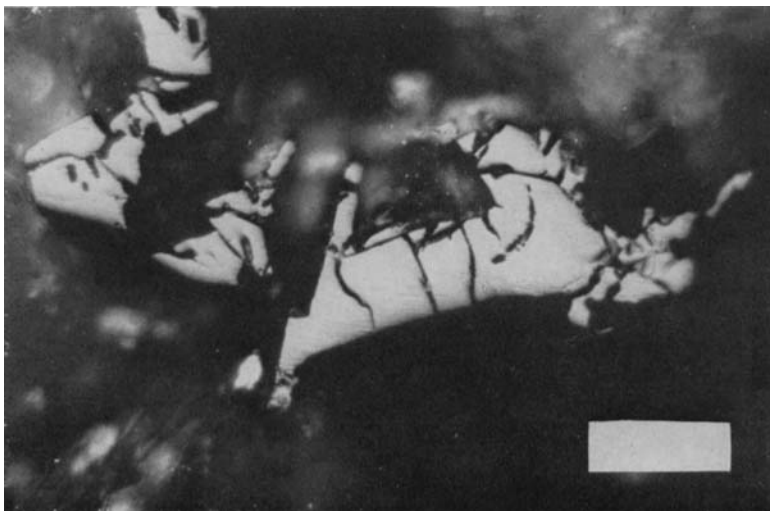

Plate 3. A titanomaghemite grain from sample 16-157-49-1 : 136 to 138. These grains show the pronounced curvilinear volume change cracks and the increased reflectivity associated with Stage 3. The lower photomicrograph shows evidence of a small amount of non-opaque material filling the void generated by the crack. The white in the upper plate is 50 μm.

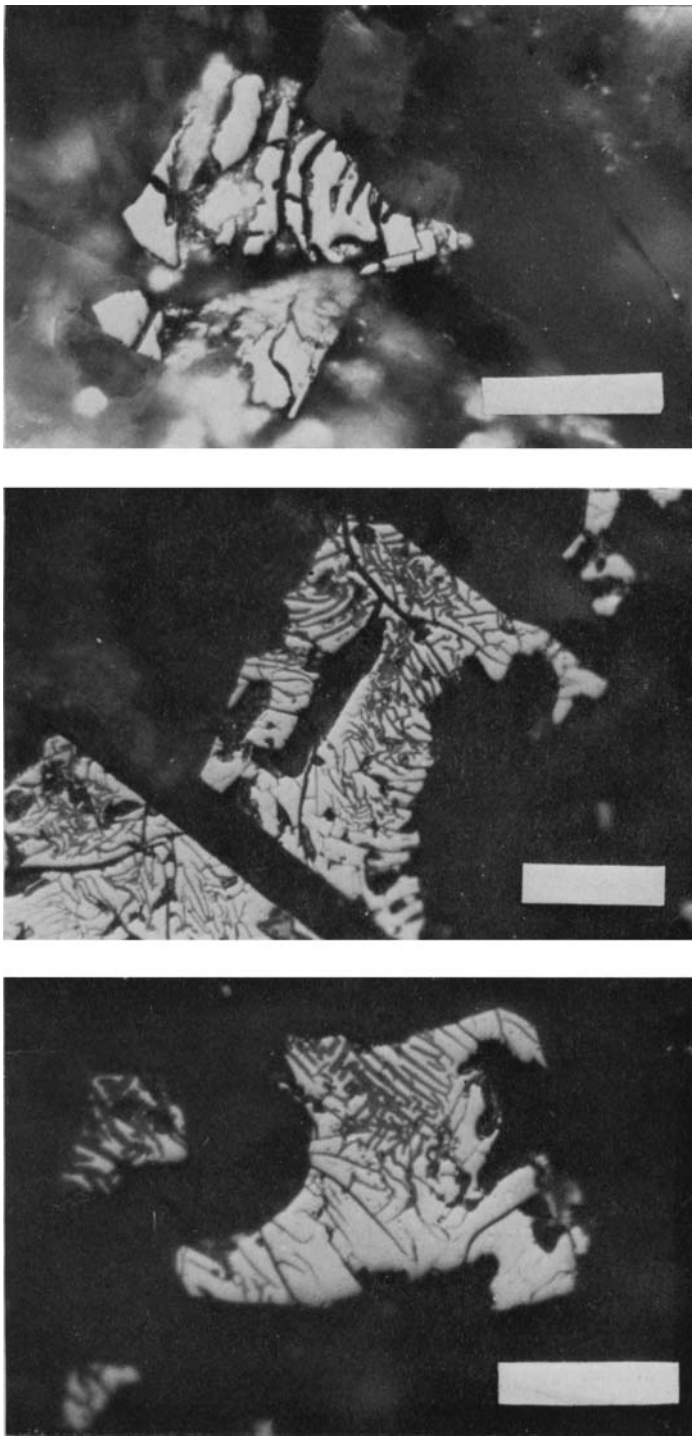

Plate 4. Three titanomaghemite grains showing the filled cracks or veins associated with Stage 4. The upper photomicrograph is from 16-157-49-1 : 136 to 138, and the lower two figures are from 34-319A-3-2: 1 08 to 111. All three grains show the replacement of the titanomaghemite phase with non-opaque materials within the veins. The upper plate shows a general eroded appearance in addition to the veins. Although not shown in the photomicrograph, the type of grains would generally be accompanied by red staining of the surrounding silicates. The length of the white bars in the three plates is 25 μm.

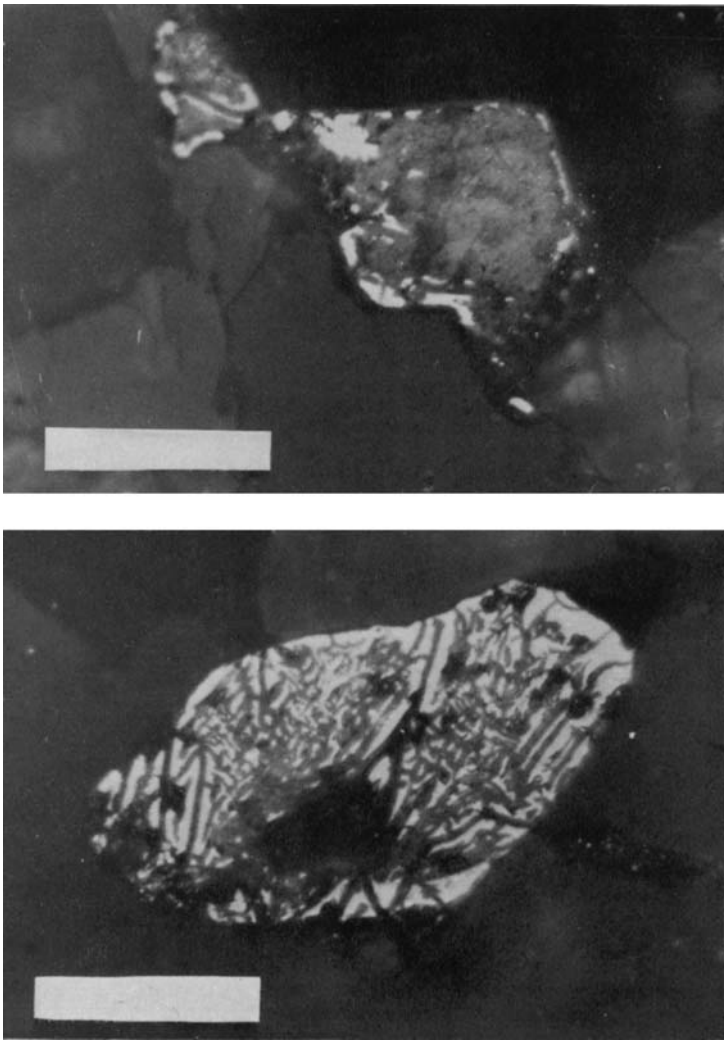

Plate 5. Two titanomaghemite grains from sample 34-319A-3-2 : 108 to 111. These grains show the eroded and replaced texture associated with the final stages of low temperature oxidation. Red staining of the surrounding silicates by, presumably, ferric oxide/hydroxide phases is common. The white bar in the upper plate is 25 μm long and in the lower figure it is 50 μm long.

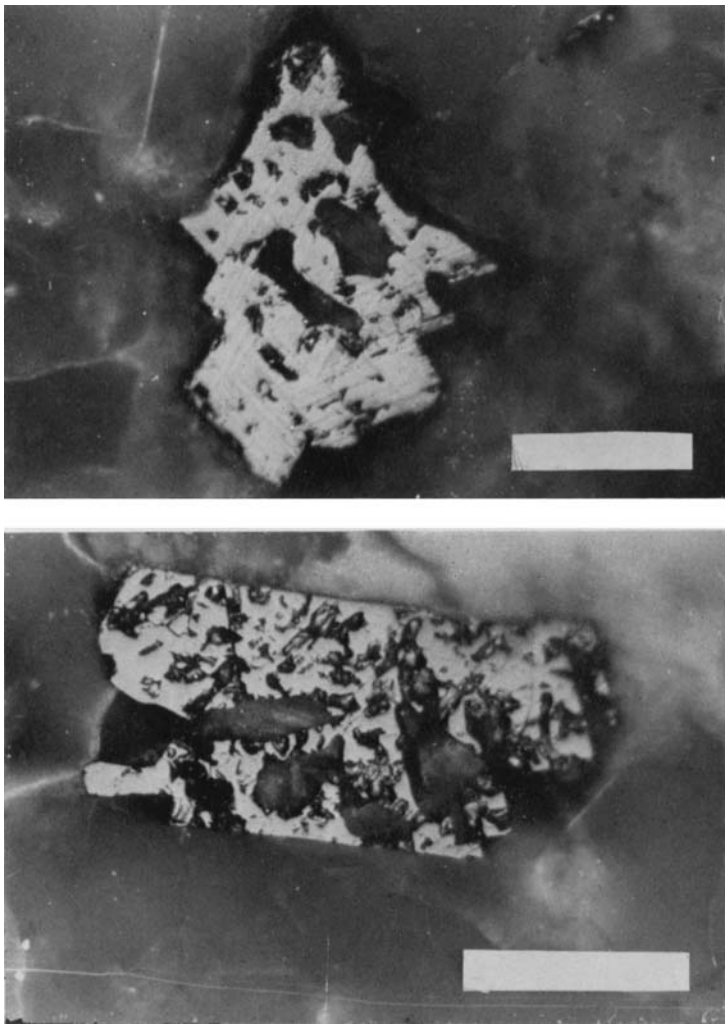

Plate 6. Two titanomagnetite grains from sample 34-319A-2-1 : 106 to 109. These grains were taken from a polished section cut perpendicular to a large vein present within a massive flow. The upper plate is a grain only 1 mm away from the vein and clearly shows the exsolved ilmenite lamellae along the (111) planes of the host magnetite, indicating the exposure to high temperature (probably deuteric) oxidation. The lower figure is a grain that is 5 mm away from the vein and shows only the high reflectivity and eroded texture associated with low temperature alteration. The white bar is 25 μm long in the upper figure and 50 μm long in the lower figure.

Figure 11. A schematic diagram illustrating the various microscopic stages of progressive low-temperature oxidation and alteration of titanomagnetite grains in submarine basalts. The dark, straight line present within the grain in Stages 1 and 2 represents a grain boundary or pre-existing structure within the grain. The fine cross-hatch marks in Stages 2 and 3 represent uneven colour changes (generally lightening) within the opaque grain.

brown-grey colour. Although the grains occasionally show cracks due to the presence of grain boundaries (or polishing scratches), the surface of the grains are largely unbroken and the grain colour is very uniform. This lack of alteration features is associated with high intensity of magnetization, low (120–150°C) Curie temperatures, and reversible $J_s(T)$ curves, indicating an unoxidized, stoichiometric titanomagnetite.

Plates 2(a) and (b) show examples of the second stage of low-temperature alteration. Small sometimes conchoidal hairline cracks, associated with the volume change of the magnetic mineral as it oxidizes, begin to appear within the grains. Some colour changes begin to occur during this stage, generally a lightening of colour to a light grey. These colour changes are not always pronounced and are not visible in these photomicrographs. Generally the Curie temperatures during this stage are between 150 and 250°C.

Plate 3 shows the third stage of oxidation where the cracks become more pronounced and there are suggestions of non-opaque material now filling the spaces between the edges

of the cracks. These pronounced low temperature oxidation cracks have been reported previously, as a general feature of low temperature oxidation (Haggerty 1976), and specifically for submarine basalts (Cockerham & Hall 1976; Ryall *et al.* 1977) and continental dike swarms (Larson & Strangway 1969). The cracks are associated with a change in volume (shrinkage) that takes place during oxidation and are related to the migration of some of the ferric cations out of the original lattice.

The colour of the grains during this stage has now become significantly lighter grey, and there are mottled zones of non-uniform colouring. As in Stage 2, these zones of lighter grey are usually found surrounding a pre-existing crack or are associated with a grain boundary. Occasionally, there is a red staining of the surrounding silicates that is associated with the titanomaghemite grains – again suggesting a migration of ferric iron cations out of the opaque grains into the surrounding ground mass. Curie temperatures for samples in this stage of oxidation seem to be usually in the intermediate range 200–300°C.

Stage 4 is represented in Plate 4(a), (b) and (c). At this point in the progressive oxidation sequence, the enlarged cracks of the previous stage are generally filled with non-opaque material and there seems to be a general erosion of the opaque grains. The remaining titanomaghemite is very bright and generally a light grey. Red staining of the ground mass is common surrounding the opaque grains. Replacement of the titanomaghemite with a dull grey phase is common, but, in some cases, the grains look eroded without obvious subsequent replacement. Curie temperatures for this stage are usually above 300°C and below 400°C but generally closer to the lower temperature.

The final stages of oxidation are shown in Plate 5(a) and (b) where the original titanomagnetite grains are largely eroded and replaced with only relics of very bright, light-grey titanomaghemite serving as indicators of the site of the original grain. Generally, the rims of the grains remain after the interiors have been completely replaced. The Curie temperature for this sample was close to the maximum temperature of 400°C that seems to be obtained for completely oxidized titanomaghemite with $x = 0.62$ (Readman & O'Reilly 1972).

Some caution should be noted in using the alteration sequence of Fig. 11 and Plates 1–5 to describe low-temperature oxidation phenomena in submarine basalts. Due to the low temperatures involved (alteration in the DSDP leg 34 samples took place at close to the seafloor ambient temperature of 4°C (Seyfried, Shanks & Bischoff 1976)) most individual samples do not show uniformly all the features of a single stage of oxidation. There was, in general, an overlap of at least two stages for each sample examined. In an extreme case, the sample shown in Plates 4 and 5 had Curie temperatures that differed by almost 100°C when chips were taken from different ends of a one-inch minicore (291 and 382°C). The schematic diagram shown in Fig. 11 is only meant as a general outline for the progressive oxidation of an individual titanomagnetite grain. A sample of low-temperature altered submarine basalt with a Curie temperature of, say, 300°C may show titanomaghemite grains with low-temperature oxidation stages of from 2 to 5 (but is unlikely to have any in Stage 1). In the low-temperature submarine environment, as is also the case for the intermediate temperature zeolite and the high-temperature deuteric oxidation ranges, non-uniformity of alteration seems to be the rule rather than the exception.

8 High-temperature oxidation

So far, the discussion of altered submarine basalts has concentrated on oxidation that occurs at temperatures of well below 100°C. At these low temperatures, the dominant oxidation product is a cation-deficient titanomaghemite. At temperatures of approximately 150°C, titanomaghemite begins to break down submicroscopically to a low-titanium magnetite phase and a rhombohedral (ilmenite) solid solution phase during laboratory oxidation (John-

son & Merrill 1973; Ryall & Ade-Hall 1975a). At oxidation temperatures between 100 and 200° for subaerially erupted basalts, this unmixing is in the form of a granulated texture, still without the formation of the characteristic ilmenite lamellae (Ade-Hall, Palmer & Hubbard 1971). At higher temperatures, presumably around 400°C and above, the ilmenite phase forms characteristic lamellae along the (111) directions of the magnetite host lattice. This oxidation sequence is probably not solely temperature dependent and will, in part, be determined by the additional presence of water and other catalytic agents.

The high-temperature form of oxidation is common in subaerial igneous rocks and has been described previously. We will be concerned here with what has been described as Class 2 and 3 (Ade-Hall, Khan & Wilson 1968; Wilson, Haggerty & Watkins 1968). The uncommon occurrence of high-temperature oxidation in the submarine basalts has been discussed in Ade-Hall *et al.* (1976). Only two of the samples from the Nazca Plate sites showed evidence of high temperature oxidation, one of them in the massive flow units of site 157 (157-49-2: 135 to 137) and one associated with a vein in a massive basalt unit in site 319 (319A-2-1: 140 to 143). In the later sample, a split minicore was taken perpendicular to the vein and one half was polished and the other half sampled for magnetic studies. This core has been discussed in detail in Ade-Hall *et al.* (1976), but Plates 6(a) and (b) show the opaque mineralogy close to the vein. Plate 6(a) was taken 1 mm from the vein and shows the clear effects of high-temperature alteration with abundant ilmenite lamellae along the (III) axes. Plate 6(b) shows a grain at a distance of 5 mm from the vein in an eroded and highly oxidized form but with no lamellae.

It would appear that while high-temperature oxidation is not common in submarine basalt, it can sometimes occur, either with deuteric alteration associated with veins or in some massive flow units. Preliminary microscopic examination of the basalt cores from DSDP leg 45 also indicates the presence of these ilmenite lamellae associated with high temperature oxidation in samples from the edges of a thick dolerite intrusion and from a highly altered breccia zone that may have been a conduit for hydrothermal circulation (Johnson 1977b).

9 Discussion

The evidence from the previous sections indicates that the rock magnetic parameters that largely control the intensity and stability of magnetic remanence in submarine basalts are: magnetic mineralogy and oxidation state, concentration of the magnetic mineral within the rock samples, and the magnetic grain size and domain state.

The predominant magnetic mineral in newly formed oceanic submarine basalts is a titanomagnetite, $Fe_{3-x}Ti_xO_4$, with a very narrow range of initial composition ($x = 0.62 \pm 0.05$). This titanomagnetite oxidizes at the ambient sea floor temperature of 4°C to a cation-deficient titanomaghemite phase.

With increasing degree of progressive low-temperature oxidation of submarine basalts:

(1) *The Curie temperature increases* from the values of 120 to 150°C for the original titanomagnetite of composition $x = 0.62$ to a maximum of 400°C for completely oxidized titanomaghemite. This rise in Curie temperature during the formation of titanomaghemite is due to the increase in exchange anisotropy energy associated with the smaller lattice size of the oxidized phase.

(2) *The saturation magnetization decreases* by more than a factor of two. There are a number of different models of cation distribution for titanomagnetites (Verhoogen 1962; O'Reilly & Banerjee 1966; Ozima & Sakamoto 1971; Readman & O'Reilly 1972) and, while all of them predict a different rate of decrease with progressive oxidation, all of them agree

with the general trend shown in Fig. 6. The errors associated with this figure are too large to allow us to distinguish between any of the models. If the decrease in Fe/Ti ratio due to iron migration out of the crystal lattice is a widespread effect, then all of the above models will be generally inapplicable to natural low-temperature oxidation.

(3) *The intensity of magnetic remanence decreases* by as much as an order of magnitude. This result is consistent with what has been observed previously in pillow basalts from mid-ocean ridges (Irving *et al.* 1970; Carmichael 1970; Marshall & Cox 1971b; Ryall & Ade-Hall 1975b; Johnson & Atwater 1977); The reduction in intensity is due, in part, to the corresponding reduction in saturation magnetization of the mineral (Fig. 6). In addition, the decrease in effective grain size by the formation of volume-change cracks and the lowering of the Fe/Ti ratio by cation migration will also play a role in the reduction in intensity of the original magnetic remanence.

(4) *The stability of magnetic remanence increases.* Since, as will be discussed later, the bulk of the grains for the samples in this study seem to be larger than single-domain size, the reduction in effective grain size by the volume-change cracks in Plates 2, 3 and 4 could be responsible for the increase in coercivity. Because of the decrease in saturation magnetization, it is unlikely that the observed increase in coercivity is due simply to a change in the contribution due to shape anisotropy. In addition to changes in effective grain size, it is likely that an increase in either the magnetocrystalline or magnetostrictive anisotropies also contribute to the increased coercivity with increasing oxidation. Since these constants have not been determined for titanomaghemites, their relative contributions are unknown.

(5) *Weak-field susceptibility decreases.* This is the result that would be expected since saturation magnetization is decreasing and coercivity is increasing with increasing oxidation. Examination of the ratio of remanent magnetization to induced magnetization, Q, indicates that, for these samples at least, the reduction of both induced and remanent magnetization occurs simultaneously and Q remains greater than unity even for highly oxidized samples (Johnson & Hall 1976).

The first two of the above categories are changes that can be solely attributed to the mineralogical changes involved in the oxidation of titanomagnetite to titanomaghemite. In the last three categories, it is impossible to sort out the effects of mineralogical changes from those associated with the effective grain size and concentration changes that result from the formation of volume change cracks.

If the effects of grain size on the magnetic properties are examined separately, looking now only at the gross grain size and not the microstructure within the grain, the following trends are apparent: with decreasing grain size, from massive flows to pillow basalts (at least down to the 2-μm limit that was observed in Fig. 8)

(1) the stability of magnetic remanence increases,
(2) the intensity of remanence decreases,
(3) weak-field susceptibility decreases and
(4) there is an increasing degree of oxidation, with the pillow basalts being much more oxidized than the massive flow material of the same age. The first three of these effects are also a consequence of their oxidation state and therefore directly related to this last category.

The effect of grain size on magnetic stability, as characterized by the median demagnetizing field, has been studied previously for titanium-free magnetite grains. Parry (1965) showed that, for grains in the size range 120–1.5 μm, the coercivity *increases* with *decreasing* grain size. Johnson, Lowrie & Kent (1975) showed that, for magnetite particles in the size range 0.2–0.015 μm, the coercivity *decreases* with *decreasing* particle size. Fig. 12 shows a composite of the data for titanium-free magnetite from Levi & Merrill (1976) and Johnson *et al.* (1975). This composite curve shows a peak in coercivity for equi-dimensional magne-

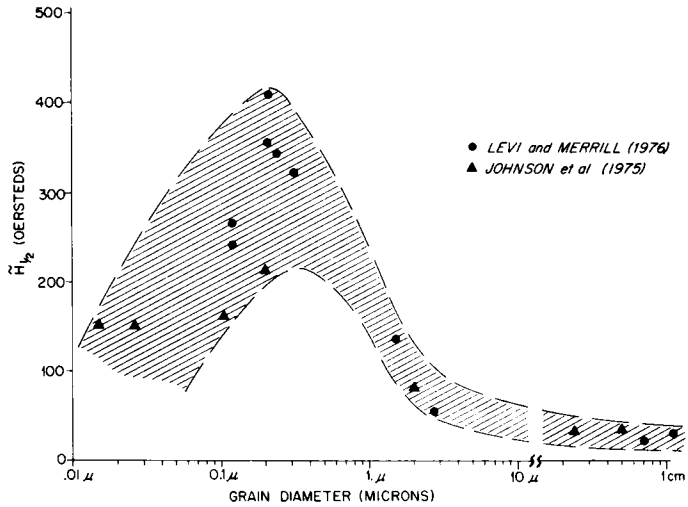

Figure 12. The dependence of coercivity of anhysteritic remanent magnetization on grain size for titanium-free magnetite cubes. With decreasing particle size, the coercivity (median demagnetizing field) rises to a maximum at about 0.2 μm and then decreases to zero. Grains less than the maximum point on the curve are single-domain and those with grain size greater than the maximum probably contain some type of pseudo-single domain or multidomain wall structure. The relatively low maximum coercivity of 400 Oe (31.8×10^3 A/m) is due to the roughly cubical size of the particles, with much higher coercivities being possible for samples with substantial shape or magnetostriction anisotropies.

tite grains at about 0.2 μm with single domain grains being to the left of the peak and grains with domain walls or wall-like structures being to the right. While it should be expected that this curve would be somewhat different for titanomagnetite grains with 65 per cent ulvospinel in solid solution, the general features of the curve of Fig. 12 are those that are required by theory and have been observed experimentally for iron, cobalt, and cobalt ferrite particles (Luborsky 1961). Comparison of the data shown in Fig. 8 with that in Fig. 12 seems to indicate that, in agreement with Soffel (1971) for samples of the same composition, the upper limit of single domain grain size is *smaller* than 1 μm. Since the bulk of the titanomagnetite grains from pillow basalts which are visible in a microscope are on the average *larger* than 1 μm (Watkins & Paster 1971; Marshall & Cox 1971a; Johnson & Atwater 1977; Ryall *et al.* 1977), it follows that most of the magnetic material in submarine basalts is larger than single domain grain size.

Studies of pillow basalts exposed on the surface of the sea floor indicate that they become extensively oxidized in a very short period of time (5×10^5 yr) (Johnson & Atwater 1977). It is interesting to note that the 15 Myr old site 319 and the 40 Myr old site 321 both have substantial amounts of unoxidized massive flow material. Since oxidation state is correlated with intensity of remanence (Figs 5 and 9), it appears that one of the major roles that grain size plays in controlling the remanent intensity is largely through the inhibition of low-temperature oxidation in the coarser grained material. It would seem that the structure and permeability of the rock units, whether as massive flows or pillow basalt, can have a more important effect on the oxidation state and magnetic properties than age alone.

In considering the relative importance of oxidation state and grain size in controlling the magnetic properties, we are faced with the classical dilemma of separation of variables. The fine-grained pillow basalts recovered so far oxidize at least two orders of magnitude faster than the coarse-grain, relatively impermeable, massive flow material. In turn, oxidation acts in reducing the effective grain size by the formation of volume change cracks within the magnetic grains. It does not seem possible to separate the two effects for individual consideration.

If the results of Table 2 can be taken as a generally applicable result, it might be useful to establish a hierarchy for pillows and massive flow units with respect to their potential ability to contribute to oceanic magnetic anomalies.

Unit	Magnetic remanence
Unoxidized pillows	Highest intensity
Unoxidized massive flows	Intermediate
Oxidized massive flows	
Oxidized pillows	Lowest intensity

As previously mentioned, studies of pillows indicate that they can pass from the state of having the highest intensity to the lowest intensity in a very short (5×10^5 yr) time. Considering the limited sampling studies so far, the massive flow units with their reduced permeability seem to oxidize at a much slower rate (greater than 40 Myr for site 321) than pillow basalts (oxidized in less than 0.5 Myr for FAMOUS area for Mid Atlantic Ridge). This would seem to suggest a mechanism for some of the two-layered, time-dependent models that have been proposed as the source of linear marine magnetic anomalies (Blakely 1976; Cande & Kent 1976). However, subsequent drilling at the Mid Atlantic Ridge (DSDP legs 37, 45, and 46) has not recovered large amounts of massive flow material, and it remains for future investigations to determine if these models are correct.

Acknowledgments

We are grateful to the shipboard scientific and technical staff of DSDP Leg 34. We thank S. Levi, S. Grommé, and K. L. Fink for permission to incorporate some of their data in our figures. D. Watson and R. Reynolds graciously made available their microscope facilities at the USGS, Golden, Colorado for some of the photomicrographs in this study. R. T. Merrill, P. Henshaw, and M. Steiner provided useful comments of earlier versions of the manuscript. This work was supported in part by the National Research Council of Canada grant A-7812 and National Science Foundation grant OCE75-21127.

Note added in proof

After the above manuscript was accepted for publication, it was brought to our attention that a sequence of low-temperature oxidation features very similar to our Fig. 11, had been previously described as occurring in the opaque minerals of Icelandic basaltic flows and dikes. The reader is referred to Hafferty (1968).

References

Ade-Hall, J. M., Fink, L. K. & Johnson, H. P., 1976. Petrography of opaque minerals, Leg 34, *Initial reports of the deep sea drilling project*, **34**, pp. 349–362, eds Hart, S. R. & Yeats, R. S., US Govt Printing Office, Washington DC.

Ade-Hall, J. M. & Johnson, H. P., 1976a. Paleomagnetism of basalts, Leg 34, *Initial reports of the deep sea drilling project*, **34**, pp. 513–532, eds Hart, S. R. & Yeats, R. S., US Govt Printing Office, Washington DC.

Ade-Hall, J. M. & Johnson, H. P., 1976b. Review of magnetic properties of basalts and sediments, Leg 34, *Initial reports of the deep sea drilling project*, **34**, pp. 769–778, eds Hart, S. R. & Yeats, R. S., US Govt Printing Office, Washington DC.

Ade-Hall, J. M., Johnson, H. P. & Ryall, P. J. C., 1976. Rock magnetism of basalts, Leg 34, *Initial reports of the deep sea drilling project*, **34**, pp. 459–468, eds Hart, S. R. & Yeats, R. S., US Govt Printing Office, Washington DC.

Ade-Hall, J. M., Khan, M. A. & Wilson, R. L., 1968. A detailed opaque petrological and magnetic investigation of a single tertiary lava from Skye, Scotland: Part 1. Iron titanium oxide petrology, *Geophys. J.*, **16**, 374–388.

Ade-Hall, J. M., Palmer, H. C. & Hubbard, T. P., 1971. The magnetic and opaque petrological response of basalts to regional hydrothermal alteration, *Geophys. J.*, **24**, 137–174.

Bence, A. E., Papike, J. J. & Ayuso, R. A., 1975. Petrology of submarine basalts from the central Caribbean. DSDP Leg 15, *J. geophys. Res.*, **80**, 4775–4804.

Blakely, R. J., 1976. An age-dependent, two-layer model for marine magnetic anomalies, *The geophysics of the Pacific Ocean basin and its margin*, pp. 227–234, eds Sutton, G. H., Manghnani, M. H. & Moberly, R., Geophysical Monograph 19, American Geophysical Union, Washington DC.

Bunch, T. E. & La Borde, R., 1976. Mineralogy and compositions of selected basalts from DSDP, Leg 34, *Initial reports of the deep sea drilling project*, **34**, pp. 263–276, eds Hart, S. R. & Yeats, R. S., US Govt Printing Office, Washington DC.

Cande, S. C. & Kent, D. V., 1976. Constraints imposed by the shape of marine magnetic anomalies on the magnetic source, *J. geophys. Res.*, **81**, 4157–4162.

Carmichael, C. M., 1970. The Mid-Atlantic Ridge near 45° N. VII. Magnetic properties and opaque mineralogy of dredged samples, *Can. J. Earth Sci.*, **7**, 239–256.

Carmichael, I. S. E. & Nicholls, J., 1967. Iron–titanium oxides and oxygen fugacities in volcanic rocks, *J. geophys. Res.*, **72**, 4665.

Cockerham, R. S. & Hall, J. M., 1976. Magnetic properties and paleomagnetism of some DSDP, Leg 33, basalts and sediment and their tectonic implications, *J. geophys. Res.*, **81**, 4207–4222.

Denham, C. R. & Guertler, J. G., 1976. Magnetic stability of eleven basalt specimens from DSDP, Leg 34, *Initial reports of the deep sea drilling project*, **34**, pp. 469–472, eds Hart, S. R. & Yeats, R. S., US Govt Printing Office, Washington DC.

Donaldson, C. H., Brown, R. W. & Reid, A. M., 1976. Petrology and chemistry of basalts from the Nazca Plate: Part 1 – Petrography and mineral chemistry, *Initial reports of the deep sea drilling project*, **34**, pp. 227–238, eds Hart, S. R. & Yeats, R. S., US Govt Printing Office, Washington DC.

Grommé, S. & Mankinen, E., 1976. Natural remanent magnetization, magnetic properties, and oxidation of titanomagnetite in basaltic rocks from DSDP, Leg 34, *Initial reports of the deep sea drilling project*, **34**, pp. 485–494, eds Hart, S. R. & Yeats, R. S., US Govt Printing Office, Washington DC.

Hall, J. M. & Ryall, P. J. C., 1977. Paleomagnetism of basement rocks, Leg 37, *Initial reports of the deep sea drilling project*, **37**, pp. 425–445, eds Aumento, F. & Melson, W. G. *et al.*

Haggerty, S. E., 1968. Fe–Ti oxides in Icelandic basic rocks and their significance in rock magnetism, *PhD thesis*, University of London.

Haggerty, S. E., 1976. Opaque mineral oxides in terrestrial igneous rocks. In *Oxide minerals, mineralogical society of America short course notes, Volume 3*, pp. 101–140, ed. Rumble, D. III, Southern Printing Company, Blackburg, Virginia, USA.

Irving, E., Park, J. K., Haggerty, S. E., Aumento, F. & Loncarevic, B. C., 1970. Magnetism and opaque mineralogy of basalts from the Mid-Atlantic Ridge at 45° N, *Nature*, **228**, 974–976.

Johnson, H. P., 1977a. Rock magnetism of oceanic crustal rocks, DSDP Leg 45, *Initial report of the deep sea drilling project*, **45**, eds Melson, W. G. & Rabinowitz, P. D., in press.

Johnson, H. P., 1977b. Paleomagnetism of oceanic crustal rocks, DSDP, Leg 45, *Initial report of the deep sea drilling project*, **45**, eds Melson, W. G. & Rabinowitz, P. D., in press.

Johnson, H. P. & Ade-Hall, J. M., 1975. Magnetic results from basalts and sediments from the Nazca Plate, *Nature*, **257**, 471–473.

Johnson, H. P. & Atwater, T., 1977. A magnetic study of the basalts from the Mid-Atlantic Ridge at 37° N, *Bull geol. Soc. Am.*, **88**, 637–647.

Johnson, H. P. & Hall, J. M., 1976. Magnetic properties of the oceanic crust: considerations from the results of DSDP, Leg 34, *J. geophys. Res.*, **81**, 5281–5293.

Johnson, H. P., Lowrie, W. & Kent, D. V., 1975. Stability of anhysteritic remanent magnetization in fine and coarse magnetite and maghemite particles, *Geophys. J. R. astr. Soc.*, **41**, 1–10.

Johnson, H. P. & Melson, W. G., 1977. Electron microprobe analyses of some titanomagnetite grains from Hole 395A, *Initial reports of the deep sea drilling project*, **45**, eds Melson, W. G. & Rabinowitz, P. D., in press.

Johnson, H. P. & Merrill, R. T., 1972. Magnetic and mineralogical changes associated with low temperature oxidation of magnetite, *J. geophys. Res.*, **77**, 334.

Johnson, H. P. & Merrill, R. T., 1973. Low temperature oxidation of a titanomagnetite and the implications for paleomagnetism, *J. geophys. Res.*, **78**, 4938.

Johnson, H. P. & Merrill, R. T., 1974. Low temperature oxidation of a single-domain magnetite, *J. geophys. Res.*, **79**, 5533–5534.

Larson, E. E. & Strangway, D. W., 1969. Magnetization of the Spanish Peaks dike swarm, Colorado and Shipwreck Dike, New Mexico, *J. geophys. Res.*, **74**, 1505–1514.

Levi, S. & Merrill, R. T., 1976. A comparison of ARM and TRM in magnetite, *Earth planet. Sci. Lett.*, **32**, 171–184.

Lowrie, W. & Kent, D. V., 1976. Viscous remanent magnetization in basalt samples, *Initial reports of the deep sea drilling project*, **34**, pp. 479–484, eds Hart, S. R. & Yeats, R. S., US Govt Printing Office, Washington DC.

Luborsky, F. E., 1961. Development of elongated particle magnets, *J. appl. Phys.*, **32**, 1715–1835.

Marshall, M. & Cox, A., 1971a. Magnetism of pillow basalts and their petrology, *Bull. geol. Soc. Am.*, **82**, 537–552.

Marshall, M. & Cox, A., 1971b. Effect of oxidation on the natural remanent magnetization of titanomagnetite in suboceanic basalt, *Nature*, **230**, 28–31.

Marshall, M. & Cox, A., 1972. Magnetic changes in pillow basalts due to sea floor weathering, *J. geophys. Res.*, **77**, 6459.

Mazzullo, L. J., Bence, A. E. & Papike, J. J., 1976. Petrography and phase chemistry of basalts from DSDP Leg 34, Nazca Plate, *Initial reports of the deep sea drilling project*, **34**, pp. 245–262, eds Hart, S. R. & Yeats, R. S., US Govt Printing Office, Washington DC.

Myers, C. W., Bence, A. E., Papike, J. J. & Ayuso, R. A., 1975. Petrology of an alkali-olivine basalt sill from Site 169 of DSDP Leg 17: the Central Pacific Basin, *J. geophys. Res.*, **80**, 807–822.

O'Reilly, W. & Banerjee, S. K., 1966. Oxidation of titanomagnetites and self-reversal, *Nature*, **211**, 26–28.

Ozima, M., Joshima, M. & Kinoshita, H., 1974. Magnetic properties of submarine basalts and the implications on the structure of the oceanic crust, *J. geomagn. Geoelect.*, **26**, 335–354.

Ozima, M. & Sakamoto, N., 1971. Magnetic properties of synthesized titanomaghemite, *J. geophys. Res.*, **67**, 7035–7046.

Ozima, M. & Ozima, M., 1971. Characteristic thermomagnetic curves in submarine basalt, *J. geophys. Res.*, **76**, 2051–2056.

Parry, L. C., 1965. Magnetic properties of dispersed magnetite powders, *Phil. Mag.*, **11**, 303–312.

Petersen, N., 1976. Notes of the variation of magnetization within basalt lava flows and dikes, *Pageoph.*, **114**, 177–193.

Prévot, M., Rémond, G. & Caye, R., 1968. Étude de la transformation d'une titanomagnétite en titanomaghémite dans une rocke volcanique, *Bull. Soc. Minéral. Cristallogr.*, **91**, 65–74.

Readman, P. W. & O'Reilly, W., 1971. Oxidation processes in titanomagnetites, *Z. Geophys.*, **37**, 329–338.

Readman, P. W. & O'Reilly, W., 1972. Magnetic properties of oxidized (cation deficient) titanomagnetites ($Fe, Ti, \square)_3O_4$), *J. geomagn. Geoelect.*, **24**, 69–90.

Ridley, W. I. & Ajdukiewicz, J., 1976. Preliminary petrology of Leg 34 basalts from the Nazca Plate, *Initial reports of the deep sea drilling project*, **34**, pp. 277–282, eds Hart, S. R. & Yeats, R. S., US Govt Printing Office, Washington DC.

Ridley, W. I., Perfit, M. R. & Adams, M. L., 1976. Petrology of basalts from the DSDP, Leg 38, *Initial reports of the deep sea drilling project*, **38**, pp. 731–730, eds Talwani, M., Vdintsev, G. *et al.*, US Govt Printing Office, Washington DC.

Ryall, P. J. C. & Ade-Hall, J. M., 1975a. Laboratory-induced self-reversal of thermoremanent magnetization in pillow basalts, *Nature*, **257**, 117–118.

Ryall, P. J. C. & Ade-Hall, J. M., 1975b. Radial variation of magnetic properties in submarine pillow basalts, *Can. J. Earth Sci.*, **12**, 1959–1969.

Ryall, P. J. C., Hall, J. M., Clark, J. & Milligan, T., 1977. Magnetization of oceanic crustal layer 2 – results and thoughts after DSDP Leg 37, *Can. J. Earth Sci.*, **14**, 684–706.

Schaeffer, R. M. & Schwarz, E. J., 1970. The Mid-Atlantic Ridge near 45° N. IX. Thermomagnetics of dredged samples of igneous rocks, *Can. J. Earth Sci.*, **7**, 268–273.

Seyfried, W. E., Shanks, W. C. & Bischoff, J. L., 1976. Alteration and vein formation in Site 321 basalts, *Initial reports of the deep sea drilling project*, **34**, pp. 385–392, eds Hart, S. R. & Yeats, R. S., US Govt Printing Office, Washington DC.

Soffel, H., 1971. The single-domain–multidomain transition in natural intermediate titanomagnetites, *Z. Geophys.*, **37**, 451–470.

Tarasiewicz, G., Tarasiewicz, E. & Harrison, C. G. A., 1976. Some magnetic properties of Leg 34 igneous rocks, *Initial reports of the deep sea drilling project*, **34**, pp. 473–478, eds Hart, S. R. & Yeats, R. S., US Govt Printing Office, Washington DC.

Verhoogen, J., 1962. Oxidation of iron–titanium oxides in igneous rocks, *J. Geol.*, **70**, 168–181.

Watkins, N. D. & Paster, T. P., 1971. The magnetic properties of igneous rocks from the ocean floor, *Phil. Trans. R. Soc. Lond. A*, **268**, 507–550.

Wilson, R. L., Haggerty, S. E. & Watkins, N. D., 1968. Variation of paleomagnetic stability and other parameters in a vertical traverse of a single Icelandic lava, *Geophys. J.*, **16**, 79–96.

Yeats, R. S., Forbes, W. C., Heath, G. R. & Scheidegger, K. E., 1973. Petrology and geochemistry of DSDP, Leg 16 basalt, Eastern Equatorial Pacific, *Initial reports of the deep sea drilling project*, **16**, pp. 617–640, eds Andel, T. H. & Heath, G. R., US Govt Printing Office, Washington DC.

Contribution No. 985, Department of Oceanography, University of Washington, Seattle, Washington 98195, USA.